


Earth Sciences

Geomorphological mapping and palaeoglacial reconstruction of the Admiralty Bay, King George Island, Maritime Antarctica

Cleiva Perondi¹, Kátia K. Rosa¹ , Jefferson C. Simões¹, Rosemary Vieira², Arthur Ayres Neto², Fabio Magrani², Carina Petsch³ and Luiz F. Velho⁴

¹Laboratório de Sedimentologia e Geomorfologia Glacial, Centro Polar e Climático, Departamento de Geografia, Universidade Federal do Rio Grande do Sul, Porto Alegre, Brazil; ²Laboratório de Processos Sedimentares e Glaciais, Instituto de Geociências, Universidade Federal Fluminense - Av. Gal. Milton Tavares de Souza, Rio de Janeiro, Brazil; ³Universidade Federal de Santa Maria, Santa Maria, Brazil and ⁴Instituto Federal de Educação Ciência e Tecnologia do Rio Grande do Sul, Porto Alegre, Brazil

Abstract

Submarine landforms in polar fjords provide essential insights into glacier responses to climate change in the Maritime Antarctic. This work aims to reconstruct the groundline of a palaeo-ice stream throughout the Holocene in Admiralty Bay, King George Island. The landforms were investigated using multi-resolution topobathymetric data based on seismic and multibeam surveys. The inner sector features shallow moraine banks and elongated glacial lineations, in contrast to the deeper moraine banks observed in the middle and outer regions of the fjord. Elongated glacial lineations indicate a north-east to south-west ice flow and a wet-based thermal regime. At ~9000 years BP, the grounding line was at the Admiralty Bay fjord's mouth. In the middle of the fjord, a prominent morainal bank reveals the palaeoglacier's grounding line. The grounding line significantly changed position after this stillstand in response to climatic variability (Mid-Holocene, at 4500–2800 years BP) and was conditioned by the deep bathymetry. The continued retreat of the ice in the Holocene possibly led to a division of the palaeo-ice stream into outlets or tidewater glaciers. MB7 and MB9 indicate the position of the grounding line during a major stillstand at the end of the inlets. The bedrock topography and fjord geometry influenced the deglaciation pattern of Dobrowolski Glacier in Martel Inlet, and the moraine banks recorded two final major stillstands. The retreat rates in Martel Inlet have increased due to the loss of anchoring points and rising temperatures after the Neoglacial period. The morainal banks present in the proximal environments at Martel Inlet are smaller, discontinuous and spaced, indicating the retreat behaviour in the last 7 decades.

Keywords: Fjord; geomorphological mapping; glacial lineation; glacial marine environment; Holocene; morainal bank; pinning points

(Received 2 September 2024; revised 20 March 2025; accepted 27 March 2025)

Introduction

Changes in polar environments in the twentieth and twenty-first centuries are associated with global and regional warming trends (Turner *et al.* 2005, Siegert *et al.* 2019). For the Antarctic Peninsula (AP) and the South Shetland Islands, such as King George Island (KGI), there is evidence of an atmospheric temperature increase greater than the global mean since 1850 CE (Siegert *et al.* 2019), promoting the progressive melting of glaciers (Dziembowski & Bialik 2022) and changes in mass balance and retreat rates, increases in ice-free areas and vegetation abundance and exposure of subglacial reliefs, among other geomorphological changes (Cuffey & Paterson 2010, Siegert *et al.* 2019).

Glaciers can serve as important proxies for reconstructing palaeoclimates at different timescales (decades to millennia). Glacier fluctuations help us to understand past, present and future climate changes. Grounding-line positions can be recorded from

morainal banks and other glacial landforms (Mackintosh *et al.* 2016). Fjords maintain relationships of terrestrial, cryospheric, oceanic and atmospheric dynamics within the Earth system. These dynamical processes occurring in fjords provide important information on how they respond to environmental modifications related to the climate (Bianchi *et al.* 2020).

Geomorphological mapping of Admiralty Bay (AB) at KGI and its surroundings could improve our understanding of proximal and distal processes at the current glacier margin and provide insightful information on the spatial configuration of glacial flow. Palaeoclimatic studies help to determine the deglaciation processes since the Last Glacial Maximum (LGM) and stillstand of the grounding line related to Neoglacial events (between 3500 and 2600–1600 years BP) and in the Little Ice Age (LIA; 1550–1800 CE). During the LGM on KGI the ice expanded onto adjacent continental shelves. The Early Climate Optimum lasted from 11 100 to 9500 years BP and was characterized by significant retreat across the AB. A prolonged cooling associated with the Neoglacial period (3000–2700 years BP) could have changed the provenance of beach deposits and environmental conditions along Joinville Island, north-eastern AP (Theilen *et al.* 2023). Simms *et al.* (2021) proposed the LIA to have significantly impacted the AP between 1550 and 1860 CE, when two major glacial advances occurred.

Corresponding author: Cleiva Perondi Email: cleivaperondi@gmail.com

Cite this article: Perondi, C., Rosa, K. K., Simões, J. C., Vieira, R., Ayres Neto, A., Magrani, F., Petsch, C., & Velho, L. F. 2025. Geomorphological mapping and palaeoglacial reconstruction of the Admiralty Bay, King George Island, Maritime Antarctica. *Antarctic Science* 37, 278–290. <https://doi.org/10.1017/S0954102025000173>

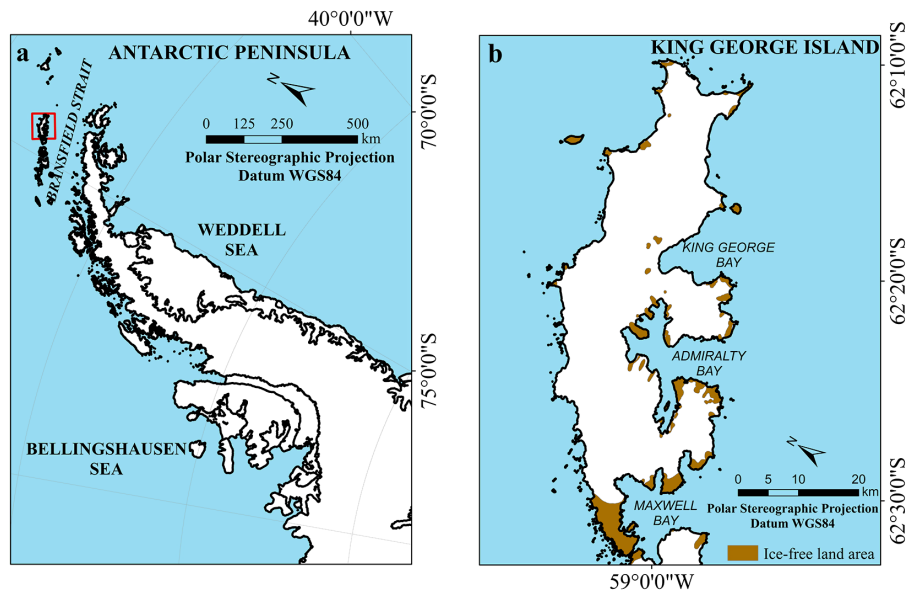


Figure 1. Localization map of Admiralty Bay, King George Island, Antarctica: **a.** Antarctic Peninsula; **b.** King George Island. Coastlines by Gerrish *et al.* (2022); Antarctic Specially Managed Area (ASMA) limits by Simões *et al.* (2001).

This work reconstructs changes in the grounding-line position, flow direction and thermal regime of glaciers as recorded by moraine ridges, morainal banks and other glacial landforms in AB throughout the Holocene.

Study area

KGI (Fig. 1) has an ice cap that flows towards the glacimarine (Bremer *et al.* 2004). AB, located on the south coast of the KGI, is an elongated fjord with steep walls and a U-shaped valley reaching depths of up to 510 m (Magrani 2014).

The mean annual air temperature is -2.8°C . In the winter months, temperatures range from -5.5°C to -1.0°C , and in the summer it ranges from -1.3°C to 2.7°C (Ferron *et al.* 2004). The region's climate is influenced by cyclones that provide rain, drizzle and snow in the summer months. However, when cyclones form in the Weddell Sea region (Fig. 1a), they bring cold air, snow and a decrease in temperature to the study area (Setzer *et al.* 2004).

Glacial retreat occurring on KGI is associated with atmospheric and ocean warming in recent decades in the AP region (Angiel & Dąbski 2012, Lorenz *et al.* 2023). Dobrowolski Glacier (2200 m in length and a maximum height of 525 m) has significantly retreated since 1950. Its area decreased from 8.2 km^2 in 1979 to 6.7 km^2 in 2021. The glacier's surface, including its thickness and height, has changed since the LIA ($\sim 4400\text{ m}$ in length and a maximum height of 550 m; Perondi *et al.* 2023).

Materials and methods

Geospatial data

The geomorphological mapping was carried out through *in situ* fieldwork and interpretation of geospatial data (Table 1). The geomorphological mapping of the glacier-free area since the 1950 sector (subaerial) analysis was carried out using the interpretation of the following geospatial data: TanDEM-X, Reference Elevation

Model of Antarctica (REMA), SPOT satellite images from 1979, 1988 and 2000, Sentinel-2 (2018 and 2020), WorldView-2 (2014) and PlanetScope (2019).

- 1) TanDEM-X: The objective of TanDEM-X/TerraSAR-X is to generate high-precision three-dimensional images of the Earth; that is, a global digital elevation model (DEM) corresponding to High Resolution Terrain Elevation, level 3 (HRTE-3), covering areas where other satellites have not obtained coherent data, with exact elevation information. The output has a 12 m spatial resolution and a vertical accuracy of less than 2 m.
- 2) REMA: REMA data are available with a spatial resolution of 2 m for almost the entire Antarctic continent. This DEM was created using sub-metre-resolution stereoscopic images obtained by WorldView-1 satellites during the summer between 2015 and 2016. Each DEM was vertically registered according to Cryosat-2 and ICESat satellites, with less than 1 m of absolute uncertainty (Howat *et al.* 2019).
- 3) Sentinel-2 images (2018 and 2020): Acquired from the United States Geological Survey (USGS) website, with a spatial resolution of 10 m and at processing level 1C.
- 4) WorldView-2 image: Obtained on 6 March 2014, with a spatial resolution of 50 cm, orthorectified and enhanced, covering an area of 60 km^2 . It was acquired at the end of the 2014 ablation season due to the absence of clouds. The WorldView-2 satellite has a spatial resolution of 50 cm.
- 5) PlanetScope image (2019): The images generated by this constellation of nanosatellites have high spatial resolution and radiometric and geometric corrections, with a daily revisit time. The image used for this work is from 2019, with a resolution of 3 m (Planet Team 2018).
- 6) Geological maps by Birkenmajer (2003) and the generation of maps of lithological units based on data from Barton (1965), Smellie *et al.* (1984, 2021) Storey (1992) and Troedson & Smellie (2002) and on Polar Rock Repository data from Matsuoka *et al.* (2021).

Table 1. Geospatial data used for the integrated geomorphological mapping of the study area. The use of data from different years and scales is due to data scarcity for Antarctica.

Sensor	Year	Spatial resolution	Data type	Source
REMA 2 and REMA 8	2018	2.2– 8.0 m	Digital elevation model (raster.tif)	Howat <i>et al.</i> (2019)
TanDEM-X	2016	12 m	Digital elevation model (raster.tif)	Braun <i>et al.</i> (2016)
GEBCO	2019	15 arcseconds	Digital elevation model (raster.tif)	GEBCO (2019)
Topobathymetric	2023	4 m	Digital elevation model (raster.tif)	Perondi <i>et al.</i> (2023)
SPOT	1979, 1988 and 2000	20 m	Satellite image	Centro Polar e Climático
Sentinel-2	2018 and 2020	10 m	Satellite image	COPERNICUS
WorldView-2	2014	0.5 m	Satellite image	UFRGS (Federal University of Rio Grande do Sul) project
PlanetScope (432 band)	2019	3 m	Satellite image	Planet Team (2018)
Shapefiles of glacier retreat	1956, 1979, 1988, 1995–2000	-	Shapefiles	Centro Polar e Climático
Shapefiles of glacier retreat, 2014	2014	-	Shapefiles	Perondi <i>et al.</i> (2019)
Shapefiles of glacier retreat, 2018	2018	-	Shapefiles	Lorenz <i>et al.</i> (2023)

GEBCO = General Bathymetric Chart of the Oceans; REMA = Reference Elevation Model of Antarctica.

- 7) Geomorphometric products: Based on the generated DEM, hypsometric, slope and aspect maps were prepared (spatial resolutions of 4 and 10 m), as well as analytical hillshade models and three-dimensional perspective scenes.

For the geomorphological mapping of the submarine environment, the following geospatial data were used: bathymetry of AB, REMA (described earlier) and the General Bathymetric Chart of the Oceans (GEBCO, 2019), along with shapefiles of frontal glacier retreat since 1956 and geomorphometric products.

- 1) Bathymetry of AB: Acoustic and bathymetric multi-resolution data were collected during three Brazilian Antarctic expeditions (OPERANTAR): OPERANTAR XXVIII (2009/2010), OPERANTAR XXXI (2012/2013) and OPERANTAR XXXII (2013/2014) aboard the Polar Ship *Admiral Maximiano* (H41), with the support of the Brazilian Navy, using Edgetech 512i sub-bottom and Kongsberg SBP 300 seismic profilers and a Simrad EM 302 multibeam echo-sounder (30 kHz frequency). The Kongsberg SBP 300 sub-bottom profiler was operated with a ping rate of 1000 ms, 2 ms pulses and a frequency envelope from 2.5 to 6.5 kHz. Magrani (2014) shows the track map with the locations of the profiler lines of the Kongsberg SBP 300 sub-bottom profiler and Edgetech 3200 surveys. The Simrad EM 302 multibeam echo-sounder aboard the SKUA boat from the Brazilian Antarctic Station Commander Ferraz was used for covering the shallower depths (including below 200 m deep) in five non-uniform spacing and parallel transects along the fjord (Perondi *et al.* 2022). The bathymetric model was generated using inverse distance weighting and based on the methodology of Ajvazi & Czimmer (2019).
- 2) GEBCO: This project aims to create a comprehensive set of nautical charts covering all seas and oceans by combining bathymetry data (GEBCO 2019). The 2019 data grid provides higher-resolution bathymetric data compared to the products from 2014. The Global Digital Elevation Model 2019 consists of a global data grid at a 15 arc-second interval, using SRTM15+ as the base version (GEBCO 2019).

Identification of the glacial landforms and geochronology

Geospatial data were integrated into a Geographic Information System (GIS) using *ArcGIS* software to identify erosional and depositional glacial landforms. The identification of landforms was based on identification criteria proposed by Bennett & Glasser (1996), Ottesen & Dowdeswell (2006), Benn & Evans (2010), Streuff *et al.* (2015) and Wölfl *et al.* (2016), which included characterizing the morphology, morphometric characteristics, depositional environment, sedimentology, genesis and the context of the glacier (parallel or perpendicular to the flow of ice). Geomorphometric data such as slope, hypsometry, shading relief and topographic profile data were used to interpret the morphology of the landforms.

For the geochronology of the environments in the study area, existing dating, changes in geomorphological and topographical aspects of the terrain and the distance from the current glacier fronts were used to infer the temporal sequence of their exposure. For the ordering of the legend, a database was created and inserted into a GIS that temporally detailed the formation and exposure of AB since the LGM, with an emphasis on the Holocene.

The geochronology of recent subaerial and submarine landforms (after 1956) was inferred based on historical data of the fluctuations of the glacier margins. For environments and features formed in periods before 1956, pre-existing dating data (Fig. 2 & Table II) and bathymetry data were used.

Results

The inner region (Fig. 3) of AB has a maximum depth of 210 m. The middle region has a maximum depth of 518.6 m and a minimum depth of 508 m. The outer region has a maximum depth of 662 m. The outer region has an average terrain slope of 10.9°, the middle region has an average terrain slope of 12.9° and the inner region has an average terrain slope of 8.9° (Fig. 3b). The highest slopes are observed between 1.0 and 1.5 km from the coast in the outer and middle regions. In the adjacent subaerial areas, the steepest sectors

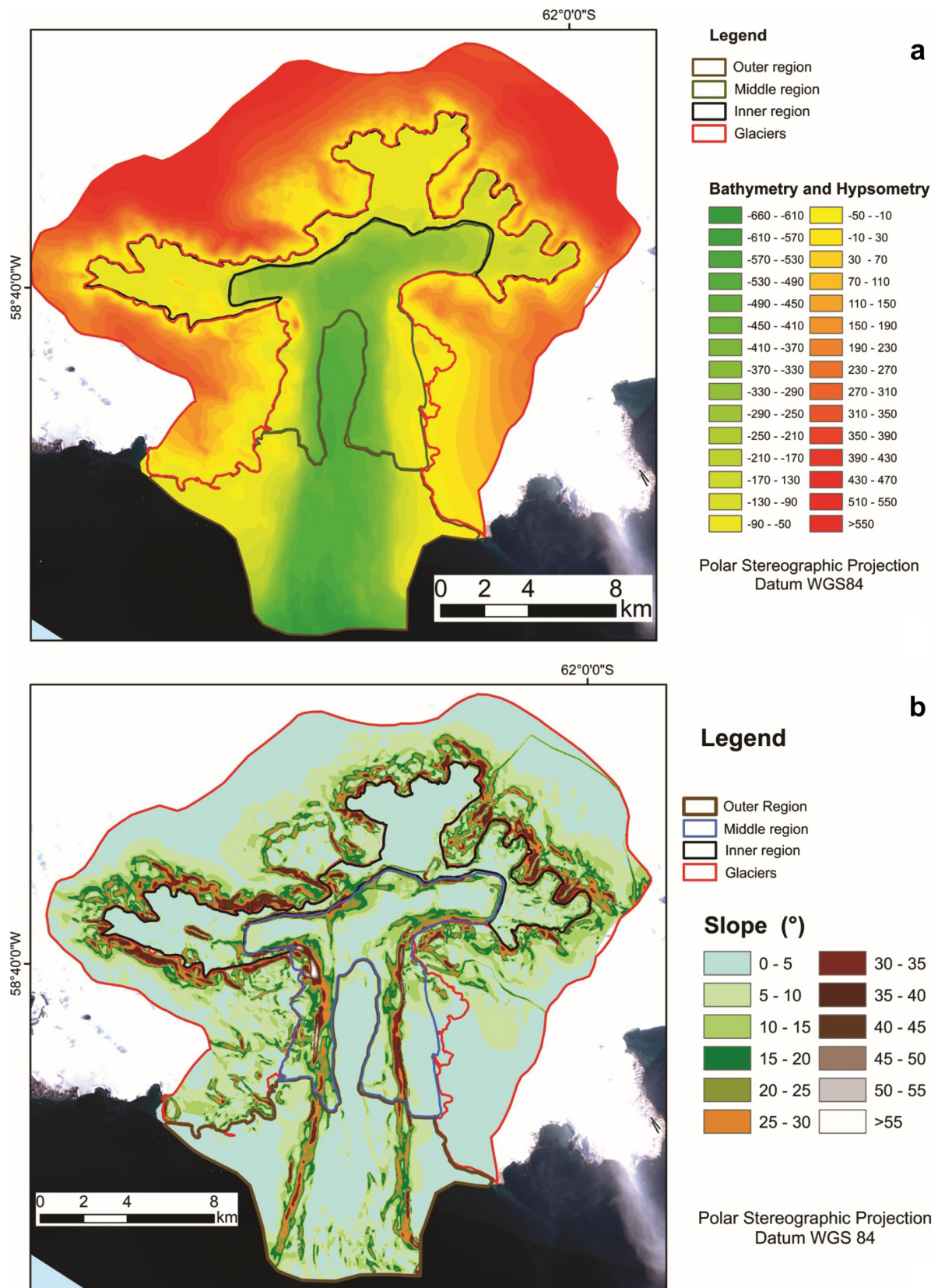


Figure 3. **a.** Hypsometric map of the study area and geochronology of the fjord environment by sector. **b.** Slope map of the study area and geochronology of the fjord environment by sector.

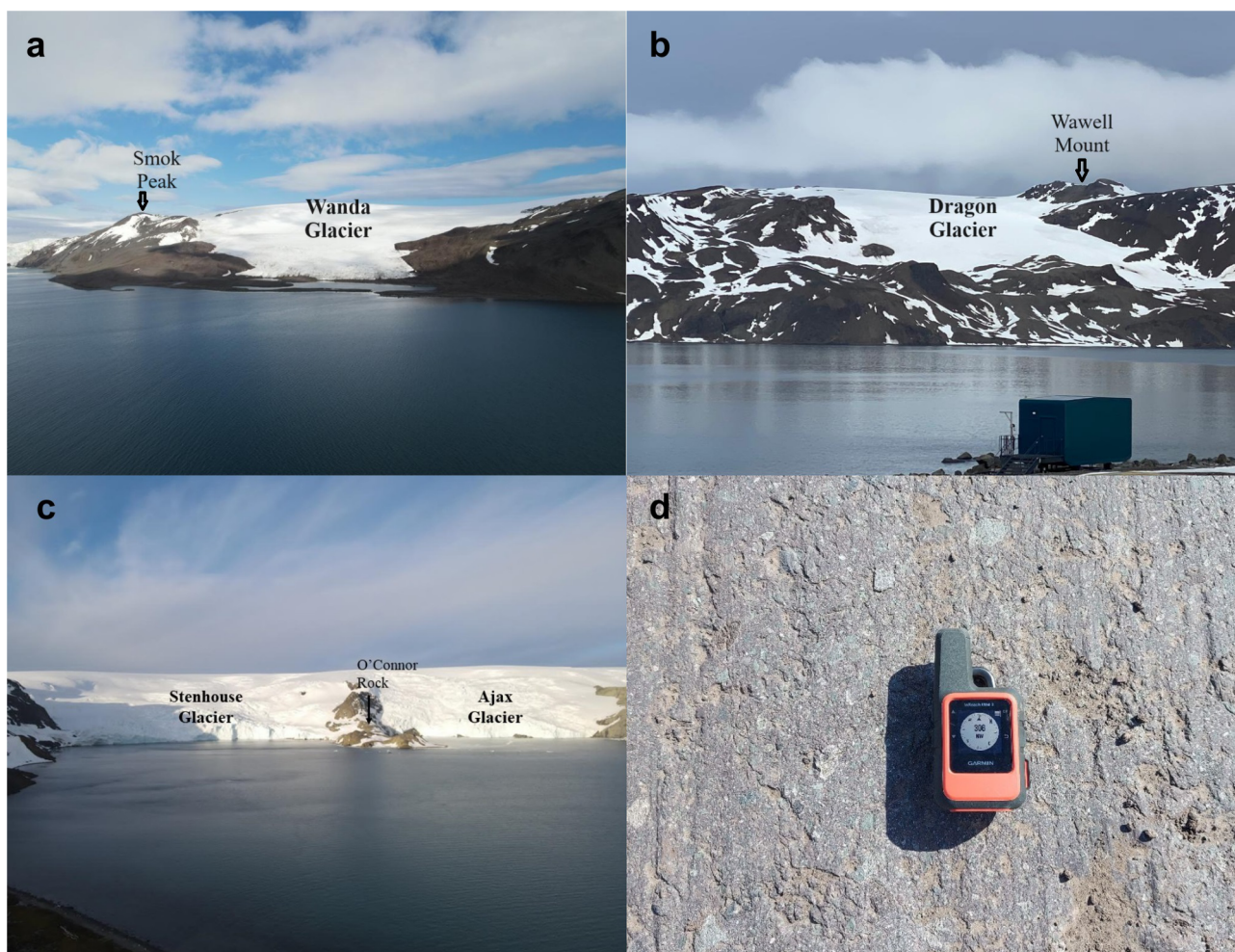


Figure 4. a. Smok Peak. b. Wawell Mount. c. O'Connor Rock. Photographs a.–c. taken by Santos Nascimento (2021). d. Striated pavement. Photograph taken by Luiz Felipe Velho and Carina Petsch (2023).

(Figs 4 & 5) and striated pavements observed at Martel Inlet (Fig. 4d).

The longitudinally aligned corrugations are most confidently interpreted as mega-scale glacial lineations. They have a north to south orientation in the outer sector. In the inner sector of Martel Inlet, these landforms have a north-east to south-west orientation (near Dobrowolski Glacier; Fig. 5). At Martel Inlet, the mega-scale glacial lineations are aligned north to south and north-north-east to south-south-west near the ice margin of the inner sector, and they change to a north-east to south-west orientation in the deep zones of the inner sector.

The morainal banks are transverse to the glacial palaeoflow of AB. Across AB, 289 morainal banks were identified. The three morainal banks, MB9 (Fig. 5 & 6), MB10 and MB7, are prominent and are located in the middle sector (Figs 5, 7 & 8). A seismic record shows a morainal bank (MB9) of ~100 m height from its seafloor base, at a depth 250 m at Ezcurra Inlet (Fig. 6).

Eskers were identified in the inner sector of Martel Inlet. They appear sinuous and are parallel to the glacial palaeoflow. An esker (ES1; Fig. 8; east to west orientation) was identified in the middle sector and is sinuous and parallel to an ancient glacial ice flow from the Kraków Icefield.

The glaciers deposited a prominent lateral morainic ridge on proglacial areas on KGI and shallow and large morainal banks (MB5, MB1 and MB3) in AB. The morainal bank MB5 (Figs 8 & 9) measures ~1.4 km in length and 8 m in height from its base (with some sections presenting lower elevations of 3–5 m) and a base width of 60 m. It is recorded at a distance of 4.4 km from the present glacial margin of Dobrowolski Glacier, at a depth of 52 m.

A feature transverse to the ice flow (MB1; Fig. 9) at ~30 m in height from its base (it can reach 60 m at some points), 675 m in length and 50 m in width is recorded at a distance of 2200 m from the ice margin (Dobrowolski Glacier). There are smaller, discontinuous and spaced morainal banks in the middle sector of deglaciation of Martel Inlet (Fig. 8). The position of the grounding line, recorded by morainal banks, was analysed to reconstruct the palaeo-ice stream glacier's extension when it occupied AB in the past (Fig. 10).

The mesoscale erosional features (linear depressions) observed in AB are most confidently interpreted as gullies. They are observed mainly on the steep slopes of Martel Inlet and in smaller quantities in AB, in the vicinity of Vieville Glacier and at the end of Mackellar Inlet. These features are small valleys observed on the fjord slope,

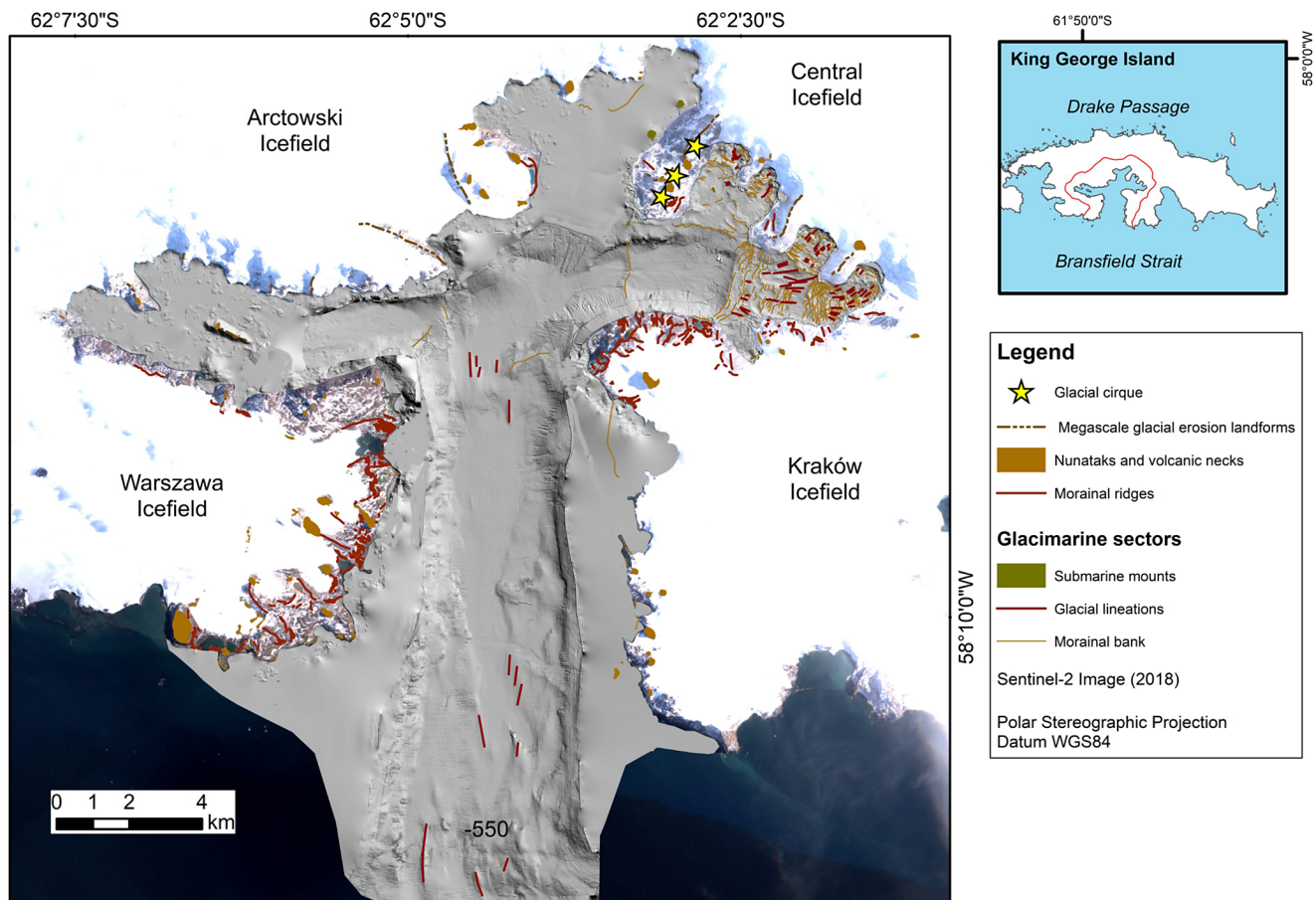


Figure 5. Geomorphological map of glacial landforms.

representing the initial stage of canyon development (Benn & Evans 2010). A palaeochannel eroded by subglacial meltwater flowing from the glacial margin to the mouth of the inlet was identified from the bathymetry data, indicating a wet basal thermal regime for the ice mass that occupied Mackellar Inlet. Magrani (2014) also identified 1 km-long submarine channels at the site, indicating the contribution of meltwater and sediments to the glacial-marine environment.

Discussion

Deglaciation of the palaeo-ice stream in the fjord

In the Early Holocene, an ice stream flowed from the highest part of the central KGI icefield, with a north-south orientation, towards AB and eroded a U-shaped valley (Fig. 5). The grounding-line position was at AB's end at 9000 years BP (Mäusbacher *et al.* 1989, Martinez-Macchiavello *et al.* 1996). Some elongated features record this palaeo-ice flow and are located at a depth of ~550 m (Fig. 5).

The outer sector has a relatively smooth valley floor compared to the sector at the head of the fjord. Marine currents, such as abyssal currents, and the accumulation of fine glacial-marine sediments, reworked particles and landforms in the deeper areas form a gentle topography.

The ice retreat on land after the deglaciation from the LGM across KGI occurred during the 11 000–8000 years BP period

(Watcham *et al.* 2011, Oliva *et al.* 2016, 2019, Heredia Barión *et al.* 2023). In AB, the deglaciation progressed and paused in the middle region. A prominent morainal bank (MB10) in AB recorded a stillstand of the grounding line. This event could be associated with a decline in atmospheric temperature at ~8000–7000 years BP, as Mulvaney *et al.* (2012) reported. The findings of Mäusbacher *et al.* (1989), Hjort *et al.* (1992) and Ingólfsson *et al.* (1992) indicate a prolonged period of decreasing mean air temperature on KGI and the advance or major stillstand of the palaeo-ice stream between 8000 and 7000 years BP. Morainal bank MB10 (depth of 450 m) is located at a fault-zone boundary over the Ezcurra Fault. Thus, there is evidence of structural conditioning.

At the time, it is inferred that the ice margin had formed a calving bay over the fjord and that the main ice flow had tributary glaciers. Locations such as Hennequin Point and Polish Navy Point (Fig. 2), today being glacier-free areas, were probably covered by ice at that time. Esker ES1, in the middle sector, indicates an ice flow in a west to east direction, following the orientation of the Kraków Fault.

The continued retreat of the palaeo-ice stream in the Holocene possibly led to the formation of the division of the palaeo-ice stream (main ice flow in a north to south direction) into glaciers with ice flows moving in east to west, north to south and west to east directions.

MB7 and MB9 indicate the positions of the grounding lines of glaciers during a major stillstand at the ends of the inlets. The grounding line at the end of Ezcurra Inlet was anchored on a

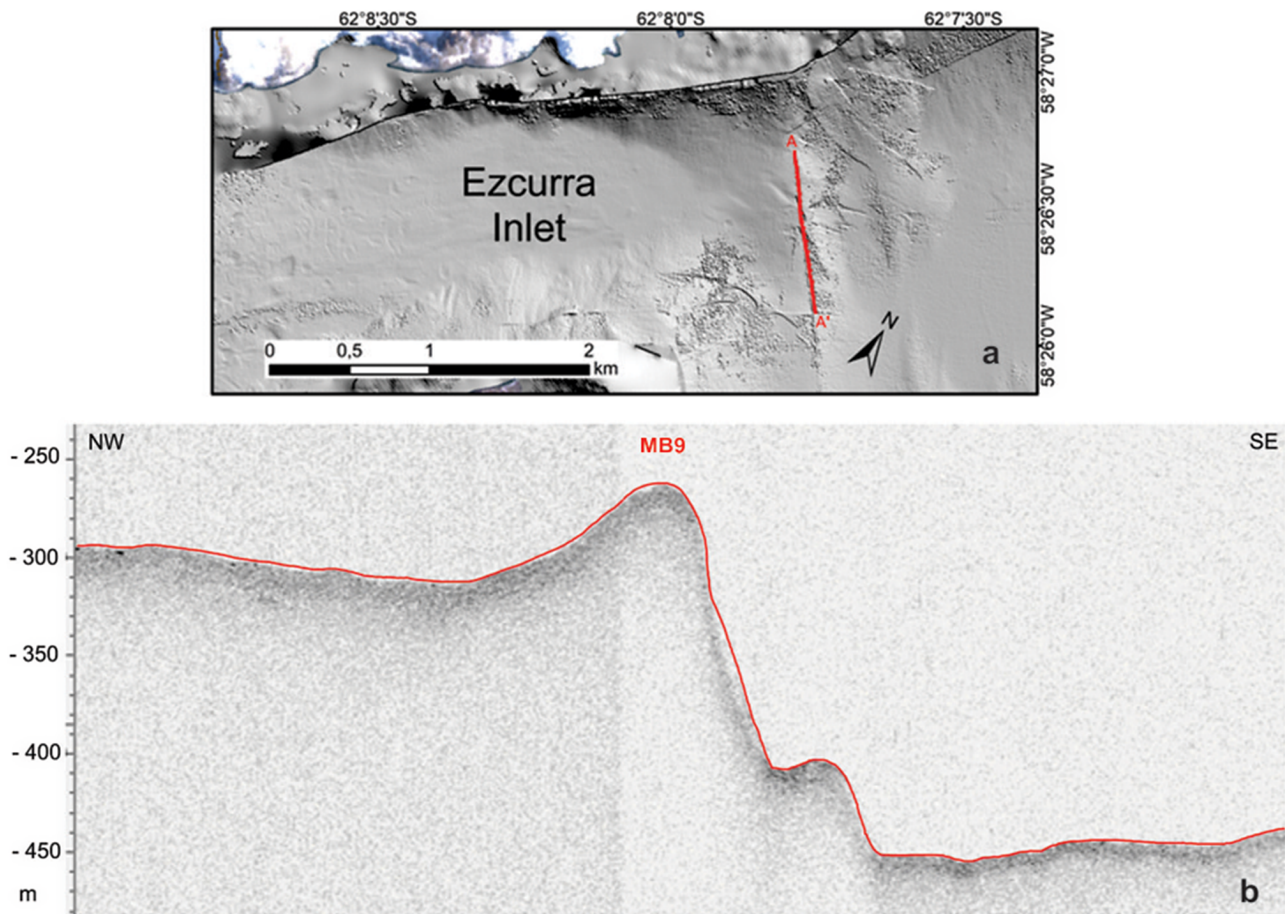


Figure 6. Morainal bank. **a.** Transect of the hill-shaded map. **b.** Seismic profile of morainal bank MB9 located at 250 m depth between Shag Rock Point and the south of Icefall Committee Glacier.

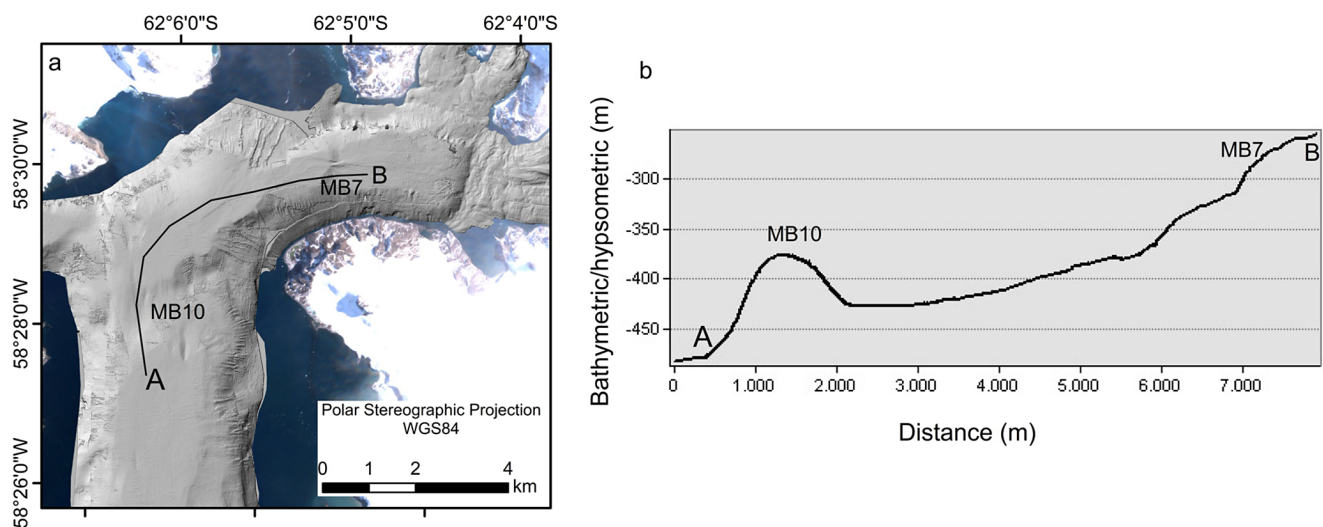


Figure 7. **a.** Transect of the hill-shaded map. **b.** Topographic profile of Admiralty Bay illustrating MB10 and MB7 in the fjord. Letter A indicates the start of the profile and B indicates the end of it.

morainal bank (MB9; Fig. 6) at 250 m deep, identified between Shag Rock Point and the south of Icefall Committee Glacier.

MB9 and MB7 mark the grounding-line positions during the stillstand and could be conditioned by the basement and

fjord geometry. Mäusbacher (1991) and Ingólfsson (2014) found evidence of glacial expansion on KGI between 5000 and 4000 years BP. Additionally, records indicate a glacial advance on Brabant Island at ~5300 years BP (Hansom & Flint 1989, Ingólfsson 2014).

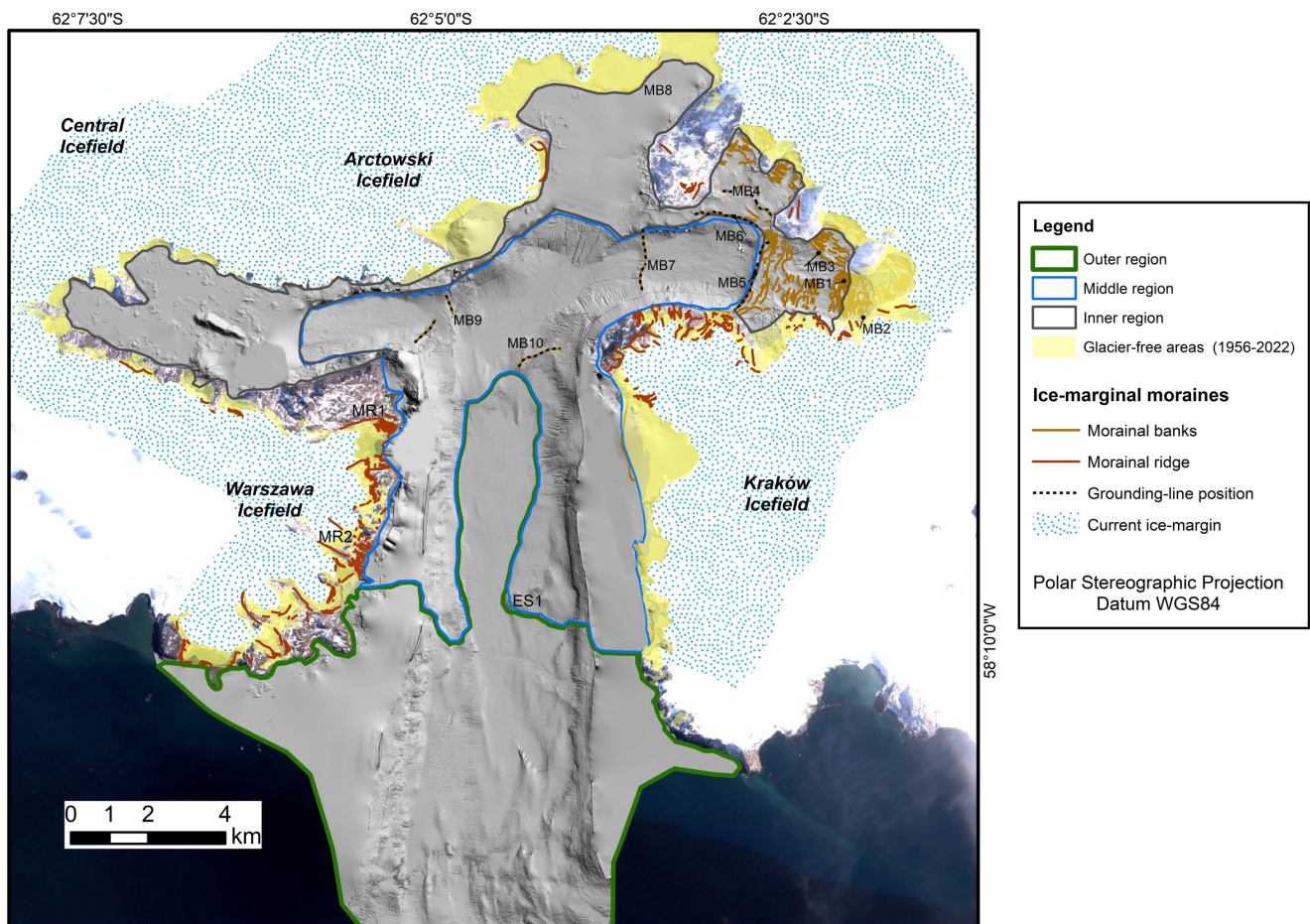


Figure 8. Evolution of the deglaciation on the fjord and morainal banks, morainic ridges (glacier-free areas) and grounding-line positions.

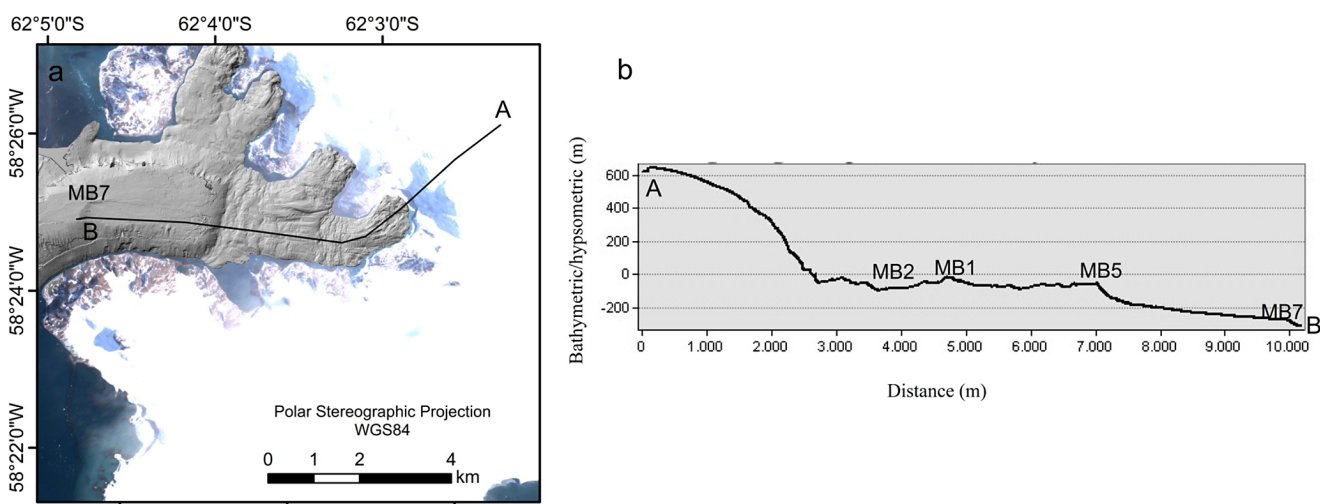


Figure 9. a. Bathymetry of Martel Inlet. b. Length of the glacial palaeoflow at 3500 years BP. Letter A indicates the start of the profile and B indicates the end of it.

For James Ross Island, the data suggest a glacial advance at ~4600 years BP (Rabassa 1983). A sediment sample collected at the mouth of Ezcurra Inlet shows at its base the presence of dropstones and larger sand grains deposited by glaciers (ice-rafted debris) shortly after a glacier advance phase; this is at the same location as MB9 (Magrani 2014).

The deglaciation of Dobrowolski Glacier in Martel Inlet

The deglaciation led to the retreat of glaciers towards the inlets in response to climatic variability (Mid-Holocene, at 4500–2800 years BP) and conditioned by the deep bathymetry. In the AP, this warm period is associated with rapid and increased marine sedimentation (Totten *et al.* 2015).

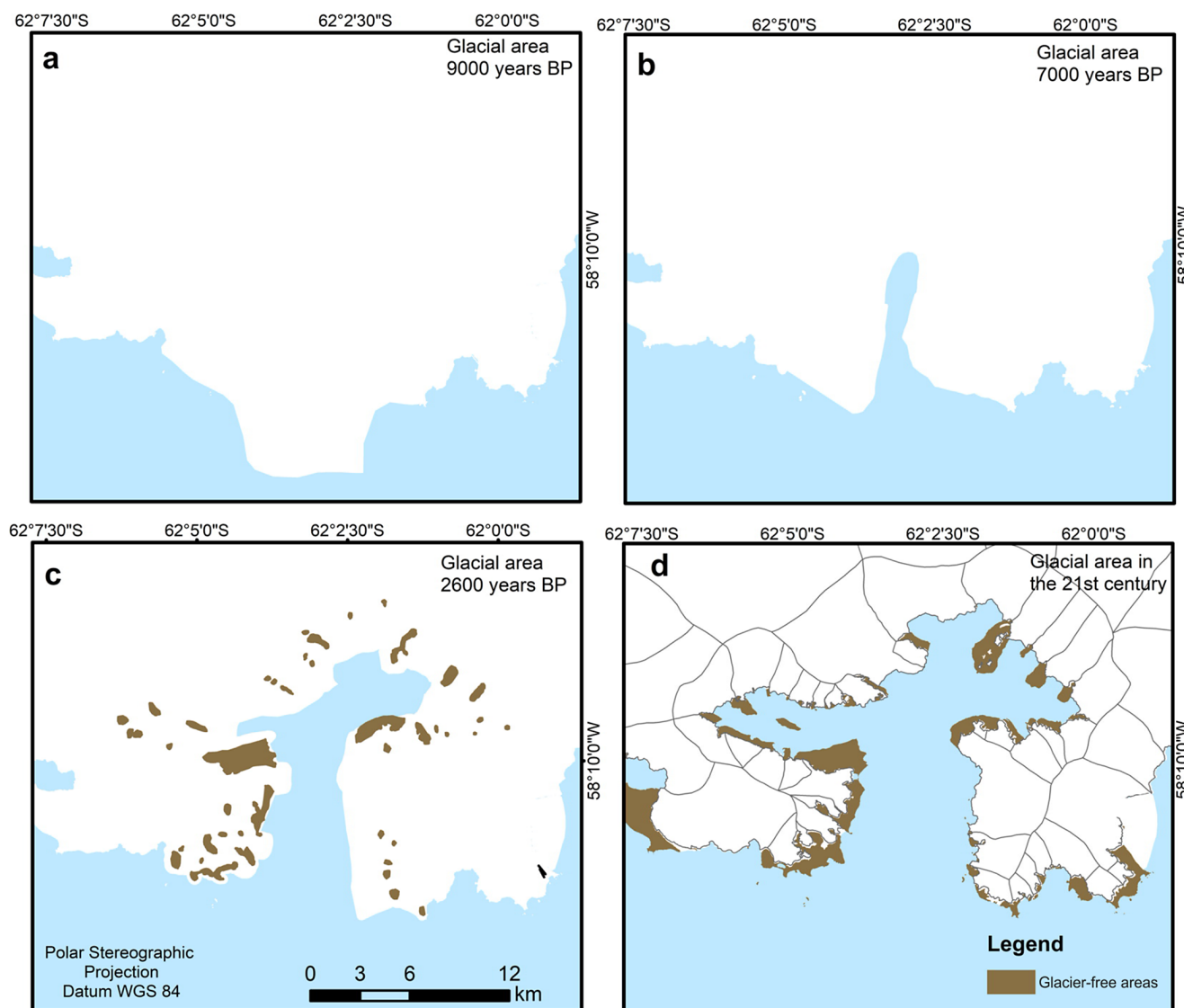


Figure 10. Reconstruction of the glacier's extension in Admiralty Bay since 9000 years BP. **a.** The ice margin at the end of the fjord. **b.** Ice-margin position during the stillstand in the middle region and the calving bay configuration. **c.** Ice-margin position during the stillstand in the inner region (Neoglacial at 2600 years BP). **d.** Glacial area in 2022.

At Martel Inlet, where the morphology is rugged compared to AB's middle region, the Dobrowolski Glacier grounding-line position (Fig. 9) was recorded by a prominent morainal bank (MB5). The distal part of the morainal bank is covered by sandy sediments and glacial debris (Magrani 2014).

The MB5 position recorded a significant stillstand, possibly in response to the decline in atmospheric and sea temperature anomalies at ~2600 years BP (Fig. 9). An anomalous bump characterizes this sector of the fjord and possibly marks the grounding-line position at 3500 years BP. Dating in moraines suggests a major advance of Collins Glacier located in Fildes Peninsula, KGI, during this period (Hall 2007, 2010). The last cooling (from 3500 to 2600 years BP) was part of a variability in climate on a millennial scale, with opposite anomalies occurring at East and West Antarctica (Mulvaney *et al.* 2012). MB5 is similar to the outermost marine moraine complex identified at Potter Cove by Wöfl *et al.* (2016) and Heredia Barión *et al.* (2023). Wöfl *et al.* (2016) argued that this feature provides evidence of the maximum position of Fourcade Glacier in the late Holocene readvance dated to ~2600–1600 years BP.

The glaciers nearby (Stenhouse and Ajax) were possibly anchored on morainal bank MB6 at depths of 50 m and at 2600 m from the ice margin. Comparatively, Wöfl *et al.* (2016) recorded an extensive morainal bank at Fourcade Glacier dated to 2600 years BP. This event was also recorded by Björck *et al.* (1993), pointing to a glacial advance on Byers Peninsula, Livingston Island, southern South Shetland Islands, due to atmospheric cooling.

The frontal moraine crest, formed near the base of Mount Flagstaff with large boulders, indicates transport over long distances by a larger glacier during a Neoglacial event with stronger drag capacity than the small cirque valley glaciers that currently occupy Keller Peninsula (Francelino 2004). The O'Connor Rock outcrop (Fig. 4c) was probably an ice divide by that time.

By 2600 years BP, the main ice-flow direction was south-east to north-west (Fig. 10c). The tributary glaciers were Goetel, Professor and Krak. The grounding line of Dobrowolski Glacier was anchored on a morainal bank (MB5) at depths between ~40 and 60 m. This glacier eroded the bedrock outcrop, forming a striated pavement (Fig. 4d). During this period, Smok Peak and Mount

Wawell (Fig. 4; elevations of 150 and 85 m, respectively) were ice divides between Wanda, Dragon and Viéville glaciers.

After 2600 years BP, Dobrowolski Glacier had retreated towards the headwaters and shallower areas of Martel Inlet. According to Yoon *et al.* (2000), a temperature increase occurred between 1900 and 1200 years BP, and the grounding line retreated to the shallower portion of Potter Cove. A sediment core collected near Dobrowolski Glacier indicates an increase in fine sedimentation after 1200 years BP, pointing to a shift to an open marine environment at this location (Yoon *et al.* 2000). Before this, sedimentation at the core site was predominantly till, which would be characteristic of an ice-contact environment.

Glacial lineation and eskers (Figs 5 & 8) indicate a wet basal thermal regime for the glaciers at ~2600 years BP. Moreover, glacial lineation indicates rapid glacial flow to Dobrowolski Glacier during this period.

A shallow and prominent morainal bank (MB1 at ~2200 m from its Dobrowolski Glacier ice margin) records the stillstand of grounding lines on KGI more recently during the LIA (~1550–1800 CE). Compared to the other glaciers, Goetel Glacier (Martel Inlet) has a more prominent morainal bank (MB3), ~1150 m from its ice margin; Stenhouse and Ajax glaciers (Martel Inlet) formed a morainal bank at 920 and 890 m away from the ice margins, respectively, during the LIA, when they were pinned and stabilized.

A long-term temperature decrease trend occurred during the 600–300 years BP period (Mulvaney *et al.* 2012, Abram *et al.* 2013), representing the LIA. Abram *et al.* (2013) noted a decrease in melting linked to this period of pronounced cooling.

The outer lateral moraine (MR1; Fig. 8), to the north of Ecology Glacier, was dated to the end of the nineteenth century, corresponding to the end of the LIA (Angiel & Dąbski 2012). Other moraines with the same location and size are laterally present on Baranowski Glacier (MR2). This scenario is attributed to the maximum glacial extension during the LIA.

The retreat of marine-terminating glaciers at Martel Inlet was influenced by fjord geometry. Stenhouse and Ajax glaciers have a higher retreat rate than the other glaciers at Martel Inlet until the 2022 grounding-line position (10D), with a few spaced morainal banks (identified from the bathymetry data given their proximity to AB; Figs 4 & 6). Stenhouse and Ajax glaciers flowed through a wider valley than Goetel and Dobrowolski glaciers. Carr *et al.* (2014) highlighted that glaciers retreat more rapidly when occupying a wider valley. A pinning point is related to a decrease in retreat rates. When the glacier loses this anchorage, the iceberg calving rate increases, leading to increased retreat (Bianchi *et al.* 2020). The increase or decrease in iceberg calving also depends on the fjord's depth and width; the calving rate is lower in narrower fjords (Carr *et al.* 2014). Tidewater glaciers tend not to respond linearly and are asynchronous to regional climatic and oceanographic signals (Motyka *et al.* 2017). Wölfl *et al.* (2016) also point to the stabilization of Fourcade Glacier due to the narrow geometry of the fjord.

Conclusions

The glacial geomorphological mapping of both the terrestrial and submarine environments of AB and adjacent glacier-free areas was interpreted, and it revealed changes in the extent, flow direction and thermal regime of palaeo-ice streams in AB and at Dobrowolski Glacier.

The grounding-line position of the palaeoglacier fluctuated in response to climate changes. The prominent morainal bank

(MB10) represents periods when the palaeoglacier's grounding line was pinned in the middle of the fjord.

The proximal parts of AB display an irregular morphology and thin layers of sedimentary deposits, with some points demonstrating bedrock outcrops. The MB1 moraine bank was established when Dobrowolski Glacier experienced a major stillstand during the LIA period. The morainal banks in the proximal environments at Martel Inlet are smaller, discontinuous and spaced, indicating the retreat pattern in recent decades.

The subglacial landforms also indicate a wet basal thermal regime. Rapid ice flow characterized the ice dynamics in the past. The glacial lineation from our records indicates active flow of the ice stream in AB during the Early Holocene.

In the submarine environment, depositional features show changes in glaciers and anchoring points at the fjord. The retreat rate in the deeper areas of the fjord was faster, as suggested by smaller or non-existent morainal banks, compared to that in the shallow areas of the fjord (inner region). After the loss of two anchoring points, the retreat rates of Dobrowolski Glacier possibly became greater in response to the warming climate trend. After the glacier's last maximum advance, recent and discontinuous moraine banks can be identified in the deglaciated area.

The glacier fluctuations responded to oceanic and climatic inputs, bedrock pinning points and the (narrow) geometry of the fjord. They were also possibly conditioned by geological structural patterns, as can be seen at Ezcurra Fault.

Acknowledgements. We thank the Postgraduate Program in Geography of the UFRGS.

Financial support. We thank the Conselho Nacional de Desenvolvimento Científico e Tecnológico (CNPq) Project 465680/2014-3 (INCT da Criosfera), Coordenação de Aperfeiçoamento de Pessoal de Nível Superior (CAPES), Brazilian Antarctic Program (PROANTAR), Observation of Research Support of the State of Rio Grande do Sul (FAPERGS) for financial support.

Competing interests. The authors declare none.

Author contributions. CIP, KKdR, CaP, FJGM and LFV: conception, approach and execution of the experiment. CIP, KKdR, FJGM and LFV: preparation of figures. CIP, CaP, KKdR, JCS, RV, AAN and FJGM: drafting of the initial manuscript and revision of the final article.

References

- ABRAM, N.J., MULVANEY, R., WOLFF, E.W., TRIEST, J., KIPFSTUHL, S., TRUSEL, L.D., *et al.* 2013. Acceleration of snow melt in an Antarctic Peninsula ice core during the twentieth century. *Nature Geoscience*, **6**, 10.1038/ngeo1787.
- AJVAZI, B. & CZIMBER, K. 2019. A comparative analysis of different DEM interpolation methods in GIS: case study of Rahovec, Kosovo. *Geodesy and Cartography*, **45**, 10.1016/j.ejrs.2013.09.001.
- ANGIEL, P.J. & DĄBSKI, M. 2012. Lichenometric ages of the Little Ice Age moraines on King George Island and the last volcanic activity on Penguin Island (West Antarctica). *Geografiska Annaler: Series A, Physical Geography*, **94**, 395–412.
- BARTON, C.M. 1965. The geology of the South Shetland Islands. III. The stratigraphy of King George Island. *British Antarctic Survey Scientific Reports*, **44**, 1–33.
- BENN, D.I. & EVANS, D.J.A. 2010. *Glaciers and glaciation*, 2nd edition. London: Hodder Arnold Publications, 816 pp.
- BENNETT, M.R. & GLASSER, N.F. 1996. *Glacial geology - ice sheets and landforms*. New York: John Wiley & Sons Ltd, 364 pp.
- BIANCHI, T.S., ARNDT, S., WILLIAN, E.N.A., BENN, D.I., BERTRAND, S., CUI, X., *et al.* 2020. Fjords as Aquatic Critical Zones (ACZs). *Earth Science Review*, **203**, 10.1016/j.earscirev.2020.103145.

- BIRKENMAJER, K. 1985. Pre-Quaternary glaciations of West Antarctica: evidence from the South Shetland Islands. *Polish Polar Research*, 3–4, 319–329.
- BIRKENMAJER, K. 2003. Admiralty Bay, King George Island (South Shetland Islands, West Antarctica): a geological monograph. *Studia Geologica Polonica*, 120, 5–73.
- BJÖRCK, S., HÅKANSSON, H., OLSSON, S., BARNEKOW, L. & JANSSENS, J. 1993. Paleoclimatic studies in South Shetland Islands, Antarctic, based on numerous stratigraphic variables in lake sediments. *Journal of Paleolimnology*, 8, 233–272.
- BRAUN, M.H., BETSCH, T. & SEEHAUS, T. 2016. *King George Island TanDEM-X DEM, link to GeoTIFF [dataset]*. Erlangen: Institut für Geographie, Friedrich-Alexander-Universität.
- BREMER, U.F., ARIGONY-NETO, J. & SIMÕES, J.C. 2004. Teledetecção de mudanças nas bacias de drenagem do gelo da ilha Rei George, Shetlands do Sul, Antártica, entre 1956 e 2000. *Pesquisa Antártica Brasileira*, 4, 37–48.
- CARR, J.R., STOKES, C. & VIELI, A. 2014. Recent retreat of major outlet glaciers on Novaya Zemlya, Russian Arctic, influenced by fjord geometry and sea-ice conditions. *Journal of Glaciology*, 60, 155–170.
- CUFFEY, K.M. & PATERSON, W.S. 2010. *Physics of glaciers*, 4th edition. Oxford: Pergamon/Elsevier, 704 pp.
- DZIEMBOWSKI, M. & BIALIK, R.J. 2022. The remotely and directly obtained results of glaciological studies on King George Island: a review. *Remote Sensing*, 14, 2736.
- FERRON, F.A., SIMÕES, J.C., AQUINO, F.E. & SETZER, A.W. 2004. Air temperature time series for King George Island, Antarctica. *Pesquisa Antártica Brasileira*, 4, 155–169.
- FRANCELINO, M.R. 2004. *Geoprocessamento aplicado ao monitoramento ambiental da Antártica Marítima: Solos, geomorfologia e cobertura vegetal na península Keller*. PhD thesis. Viçosa: Universidade Federal de Viçosa, 114 pp.
- GEBCO. 2019. *GEBCO 2019 Grid*. Retrieved from: https://www.bodc.ac.uk/data/published_data_library/catalogue/10.5285/836f016a-33be-6ddc-e053-6c86abc0788e
- GERRISH, L., FRETWELL, P. & COOPER, P. 2022. *High resolution vector polylines of the Antarctic coastline (7.5) [dataset]*. Cambridge: UK Polar Data Centre, Natural Environment Research Council, UK Research & Innovation.
- HALL, B.L. 2007. Late-Holocene advance of the Collins Ice Cap, King George Island, South Shetland Islands. *Holocene*, 17, 10.1177/0959683607085132.
- HALL, B.L. 2010. Holocene relative sea-level changes and ice fluctuations in the South Shetland Islands. *Global Planetary Change*, 74, 10.1016/j.gloplacha.2010.07.007.
- HANSOM, J.D. & FLINT, C.P. 1989. Short notes. Holocene ice fluctuations on Brabant Island, Antarctic Peninsula. *Antarctic Science*, 1, 165–166.
- HEREDIA BARIÓN, P.A., STRELIN, J.A., ROBERTS, S.J., SPIEGEL, C., WACKER, L., NIDERMAN, S., et al. 2023. The impact of Holocene deglaciation and glacial dynamics on the landscapes and geomorphology of Potter Peninsula, King George Island (Isla 25 Mayo), NW Antarctic Peninsula. *Frontier Earth Science*, 10, 10.3389/feart.2022.1073075.
- HJORT, C., INGÓLFSSON, O. & BJÖRCK, S. 1992. The last major deglaciation in the Antarctic Peninsula region. A review of recent Swedish Quaternary research. In YOSHIDA, Y., KAMINUMA, K. & SHIRAISHI, K., eds, *Recent progress in Antarctic Earth science*. Tokyo: Terra Scientific Publishing Company, 741–743.
- HOWAT, I.M., PORTER, C., SMITH, B.E., NOH, M.J. & MORIN, P. 2019. The Reference Elevation Model of Antarctica. *The Cryosphere*, 13, 665–674.
- INGÓLFSSON, Ó. 2014. Late Quaternary glaciation of Antarctica. In *Reference Module in Earth Systems and Environmental Sciences*. Amsterdam: Elsevier, 10.1016/b978-0-12-409548-9.09430-6.
- INGÓLFSSON, Ó., HJORT, C., BJÖRCK, S. & SMITH, R. 1992. Late Pleistocene and Holocene glacial history of James Ross Island, Antarctic Peninsula. *Boreas*, 21, 198–222.
- LORENZ, J., ROSA, K.K., PETSCH, C., PERONDI, C., IDALINO, F., AUGER, J., et al. 2023. Short-term glacier area changes, glacier geometry dependence, and regional climatic variations forcing, King George Island, Antarctica. *Anais da Academia Brasileira de Ciências*, 95, 1–26.
- MACKINTOSH, A.N., ANDERSON, B.M. & PIERREHUMBERT, R.T. 2016. Reconstructing climate from glaciers. *Annual Review of Earth and Planetary Sciences*, 45, 649–680.
- MAGRANI, F. 2014. *Caracterização sedimentar glaciomarinha da deglaciação da BA desde o Último Máximo Glacial, arquipélago das Shetlands Do Sul, Antártica*. MSc dissertation. Niterói: Universidade Federal Fluminense, 198 pp.
- MARTINEZ-MACCHIAVELLO, J.C., TATUR, A., SERVANT-VILDARY S. & DEL VALLE, R. 1996. Holocene environmental change in a marine-estuarine-lacustrine sediment sequence, King George Island, South Shetland Islands. *Antarctic Science*, 8, 313–322.
- MATSUOKA, K., SKOGLUND, A., ROTH, G., POMEREU, J., GRIFFITHS, H., HEADLAND, R., et al. 2021. *Quantarctica*, an integrated mapping environment for Antarctica, the Southern Ocean, and sub-Antarctic islands. *Environmental Modelling & Software*, 140, 10.1016/j.envsoft.2021.105015.
- MÄUSBACHER, R. 1991. Die Jungkvartäre Relief und Klimageschichte im Bereich der Fildeshalbinsel, Süd-Shetland-Inseln, Antarktis. *Heidelberger Geographische Arbeiten*, 89, 1–207.
- MÄUSBACHER, R., MÜLLER, J., MUNNICH, M. & SCHMIDT, R. 1989. Evolution of postglacial sedimentation in Antarctic lakes (King George Island). *Zeitschrift für Geomorphologie*, 33, 219–234.
- MOTYKA, R.J., CASSOTTO, R., TRUFFER, M., KJELDSEN, K.K., VAN, A.S.D., KORSGAARD, N.J., et al. 2017. Asynchronous behavior of outlet glaciers feeding Godthabsfjord (Nuup Kangerlua) and the triggering of Narsap Sermiá's retreat in SW Greenland. *Journal of Glaciology*, 63, 10.1017/jog.2016.138.
- MULVANEY, R., ABRAM, N.J., HINDMARSH, R.C.A., ARROWSMITH, C., FLEET, L., TRIEST, J., et al. 2012. Recent Antarctic Peninsula warming relative to Holocene climate and ice-shelf history. *Nature*, 489, 141–144.
- Ó COFAIGH, C., DAVIES, B.J., LIVINGSTONE, S.J., SMITH, J.A., JOHNSON, J.S., HOCKING, E.P., et al. 2014. Reconstruction of ice-sheet changes in the Antarctic Peninsula since the Last Glacial Maximum. *Quaternary Science Review*, 100, 10.1016/j.quascirev.2014.06.023.
- OLIVA, M., ANTONIADES, D., GIRALT, S., GRANADOS, I., PLA-RABES, S., TORO, M., et al. 2016. The Holocene deglaciation of the Byers Peninsula (Livingston Island, Antarctica) based on the dating of lake sedimentary records. *Geomorphology*, 261, 10.1016/j.geomorph.2016.02.029.
- OLIVA, M., ANTONIADES, D., SERRANO, E., GIRALT, S., LIU, E.J., GRANADOS, I., et al. 2019. The deglaciation of Barton peninsula (King George Island, South Shetland Islands, Antarctica) based on geomorphological evidence and lacustrine records. *Polar Records*, 55, 10.1017/s0032247419000469.
- OTTESEN, D. & DOWDESWELL, J.A. 2006. Assemblages of submarine landforms produced by tidewater glaciers in Svalbard. *Journal of Geophysical Research*, 111, 10.1029/2005JF000330.
- PERONDI, C., ROSA, K.K. & VIEIRA, R. 2019. Caracterização geomorfológica das áreas livres de gelo na margem leste do campo de gelo Warszawa, ilha Rei George, Antártica Marítima. *Revista Brasileira de Geomorfologia*, 20, 10.20502/rbg.v20i2.1433.
- PERONDI, C., ROSA, K.K., VIEIRA, R., MAGRANI, F.J.G., AYERS-NETO, A. & SIMÕES, J.C. 2022. Geomorphology of Martel Inlet, King George Island, Antarctica: a new interpretation based on multi-resolution topo-bathymetric data. *Anais da Academia Brasileira de Ciências*, 94, 10.1590/0001-376520220210482.
- PERONDI, C., ROSA, K.K., MAGRANI, F., PETSCH, C., VIEIRA, R., AYERS-NETO, A. & SIMÕES, J.C. 2023. Paleoglaciological reconstruction and geomorphological mapping of Dobrowolski Glacier, King George Island, Antarctica. *Revista Brasileira de Geomorfologia*, 24, 10.20502/rbg.v24i3.2425.
- PLANET TEAM. 2018. *Planet Imagery Product Specification 2018*. San Francisco, CA: Planet Labs, Inc. Retrieved from <https://www.nrs.gov.in/sites/default/files/pdf/foreigndata/planetscope1.pdf>
- RABASSA, J. 1983. Stratigraphy of the glacial deposits in northern James Ross Island, Antarctic Peninsula. In EVENSON, E., SCLUCHTER, C. and RABASSA, J., eds, *Tills and related deposits*. Rotterdam: A. A. Balkema Publishers, 329–340.
- SETZER, A.W.O., FRANCELINO, M.R., SCHAFFER, C.E.G.R., COSTA, L.V. & BREMER, U.F. 2004. Regime climático na Baía do Almirantado: relações com o ecossistema terrestre. In SCHAEFER, C., ed., *Ecossistemas costeiros e monitoramento ambiental da Antártica Marítima Monograph*. Minas Gerais: Viçosa, 1–13.
- SIEGERT, M., ATKINSON, A., BANWELL, A., BRANDON, M., CONVEY, P., DAVIES, B., et al. 2019. The Antarctic Peninsula under a 1.5°C global warming scenario. *Frontiers in Environmental Science*, 7, 10.3389/fevs.2019.00102.
- SIMMS, A.R., BENTLEY, M., SIMKINS, L., ZURBUCHEN, J., REYNOLDS, L., DEWITT, R., et al. 2021. Evidence for a 'Little Ice Age' glacial advance within the

- Antarctic Peninsula: examples from glacially overrun raised beaches. *Quaternary Science Review*, **271**, 10.1016/j.quascirev.2021.107195.
- SIMÕES, J.C., FERRON, F.A., BRAUN, M., ARIGONY, J. & AQUINO, F.E. 2001. A GIS for the Antarctic Specially Managed Area of Admiralty Bay, King George Island, Antarctica. *Geo-spatial Information Science*, **4**, 8–14.
- SMELLIE, J.L., HUNT, R.J., MCINTOSH, W.C. & ESSER, R.P. 2021. Lithostratigraphy, age and distribution of Eocene volcanic sequences on eastern King George Island, South Shetland Islands, Antarctica. *Antarctic Science*, **33**, 10.1017/S0954102021000213.
- SMELLIE, J.L., PANKHURST, R.J., THOMSON, M.R.A. & DAVIES, R.E.S. 1984. The geology of the South Shetland Islands: VI. Stratigraphy, geochemistry and evolution. *British Antarctic Survey Scientific Reports*, **87**, 1–85.
- STOREY, B. 1992. Commentary on schematic geological map of Antarctica 1:10 000 000. *Antarctic Science*, **4**, 10.1017/S0954102092230388.
- STREUFF, K., FORWICK, M., SZCZUCINSKI, W., ANDREASSEN, K. & Ó COFAIGH, C. 2015. Submarine landform assemblages and sedimentary processes related to glacier surging in Kongsfjorden, Svalbard. *ArKtos*, **1**, 10.1007/s41063-015-0003-y.
- TATUR, A., DEL VALLE, R. & BARCZUK, A. 1999. Discussion on the uniform pattern of Holocene tephrochronology in South Shetland Islands, Antarctica. *Polish Polar Studies*, **1**, 303–321.
- THEILEN, B.M., GARCIA, A.R.S.C., DEWITT, R., ZURBUCHEN, J. & GERNANT, C. 2023. The impact of the Neoglacial and other environmental changes on the raised beaches of Joinville Island, Antarctica. *Antarctic Science*, **35**, 10.1017/S0954102023000275.
- TOTTEN, R.L., ANDERSON, J.B., FERNANDEZ-VASQUEZ, R.A. & WELLNER, J.S. 2015. Marine record of Holocene climate, ocean, and cryosphere interactions: Herbert Sound, James Ross Island, Antarctica. *Quaternary Science Reviews*, **129**, 10.1016/j.quascirev.2015.09.009.
- TROEDSON, A.L. & SMELLIE, J.L. 2002. The Polonez Cove Formation of King George Island, Antarctica: stratigraphy, facies and implications for mid-Cenozoic cryosphere development. *Sedimentology*, **49**, 277–301.
- TURNER, J., LACHLAN-COPE, T., COLWELL, S. & MARSHALL, G.J. 2005. A positive trend in Western Antarctic Peninsula precipitation over the last 50 years reflecting regional and Antarctic-wide atmospheric circulation changes. *Annals Glaciology*, **41**, 10.3189/172756405781813177.
- WATCHAM, E.P., BENTLEY, M.J., HODGSON, D.A., ROBERTS, S., FRETWELL, P., LLOYD, J., *et al.* 2011. A new Holocene relative sea level curve for the South Shetland Islands, Antarctica. *Quaternary Science Review*, **30**, 10.1016/j.quascirev.2011.07.021.
- WÖFL, A.C., WITTENBERG, N., FELDENS, P., HASS, H.C., BETZLER, C. & KUHN, G. 2016. Submarine landforms related to glacier retreat in a shallow Antarctic fjord. *Antarctic Science*, **28**, 10.1017/S0954102016000262.
- YOON, H.H., PARK, B.K., KIM, Y. & KIM, D. 2000. Glaciomarine sedimentation and its palaeoceanographic implications along the fiord margins in the South Shetland Islands, Antarctica during the last 6000 years. *Paleogeography, Palaeoclimatology, Paleoecology*, **157**, 189–211.